Non-dissipative tunnelling between low-dimensional electron states in a magnetic field

1996 J. Phys.: Condens. Matter 8 1041

(http://iopscience.iop.org/0953-8984/8/8/014)

J. Phys.: Condens. Matter **8** (1996) 1041–1050. Printed in the UK

Non-dissipative tunnelling between low-dimensional electron states in a magnetic field

O E Raichev and F T Vasko

Institute of Semiconductor Physics, NAS Ukraine, Prospect Nauki 45, Kiev-28, 252650, Ukraine†

Received 1 September 1995, in final form 27 October 1995

Abstract. We calculate the tunnelling current between spatially separated low-dimensional electron layers in conditions where the magnetic field is applied perpendicular to the tunnelling direction. Due to the magnetic-field-induced intersection of the parabolic electron spectrum branches, the current is independent of the scattering mechanism over a wide region of magnetic field, applied voltage, and level splitting, i.e. the non-dissipative tunnelling regime is realized. We derive expressions for the tunnelling rate and tunnel current in coupled quantum wells and wires, and compare these results with the existing experimental data concerning the photoexcited electron relaxation in double quantum wells, and tunnelling between the two-dimensional and quasi-one-dimensional layers with independent contacts to each layer. Good agreement between the theory and the experiments indicates realization of the non-dissipative tunnelling regime in all of the cases considered.

1. Introduction

In contrast to the tunnelling of electrons in bulk media, the tunnelling between low-dimensional electron systems must be assisted by a scattering in order to satisfy the momentum and energy conservation requirements. For example, the tunnelling event in double quantum wells (DQWs) and other spatially separated two-dimensional (2D) structures [1] includes the momentum (or the momentum and energy) transfer needed for a transition from one parabolic branch of the electron spectrum to another; see figure 1(a). When the level-splitting energy Δ (which is usually controlled by a transverse electric field) is much larger than the collision broadening energy $\hbar/\tau$ (τ is the scattering time), the tunnelling probability is proportional to the scattering rate τ^{-1}. In conditions of tunnelling resonance, when $\Delta \ll \hbar/\tau$, this probability is proportional to τ [2], i.e. the tunnel current depends on the scattering time in the same way as does the electric current in conducting media. The same situation (see figure 2(a)) is found in tunnelling between quantum wires formed by application of a lateral confinement potential to the DQWs or related structures [3]. It is important that in all these cases the tunnelling is dissipative and its probability is explicitly expressed through the quantities characterizing the scattering.

A basically new situation is found when the magnetic field $\boldsymbol{H}$ is applied perpendicular to the tunnelling direction (the z axis); below we always assume that $\boldsymbol{H}$ is parallel to the y axis. The influence of the magnetic field on the electron spectrum in DQWs manifests itself as a field-dependent shift [4] of the 2D energy spectra $\varepsilon_l(\boldsymbol{p})$ and $\varepsilon_r(\boldsymbol{p})$ in the right-hand

† E-mail: zinovi@lab2.kiev.ua.

0953-8984/96/081041+10$19.50

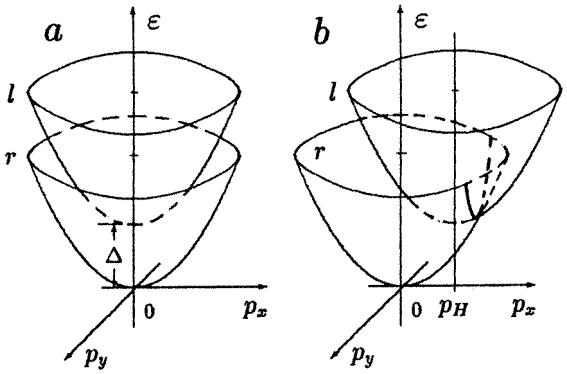

Figure 1. The electron spectrum in double quantum wells: (*a*) without the magnetic field; (*b*) with the magnetic field applied parallel to the 2D layers (along the *y* axis).

(*r*-) and left-hand (*l*-) wells with respect to each other, as shown in figure 1(*b*). As a result, the spectra intersect each other in the momentum–energy space. The electron transition from one branch to another in the vicinity of the intersection does not require scattering, so the tunnelling can proceed in a non-dissipative way. An analogous case can be realized in the above-described quantum wires, when the magnetic field is applied perpendicular both to the tunnelling direction and to the wire direction (the *x* axis). The shift of the quasi-one-dimensional (1D) spectra belonging to the *l*- and *r*-layers is shown in figure 2(*b*)). The intersection takes place at a number of *points* in the momentum–energy plane (in contrast to in the 2D case, when the intersection occurs in a *line*; see figure 1(*b*)). Again, the tunnelling between quasi-1D states near the intersections is non-dissipative.

Investigation of the tunnelling between 2D states in the presence of a magnetic field

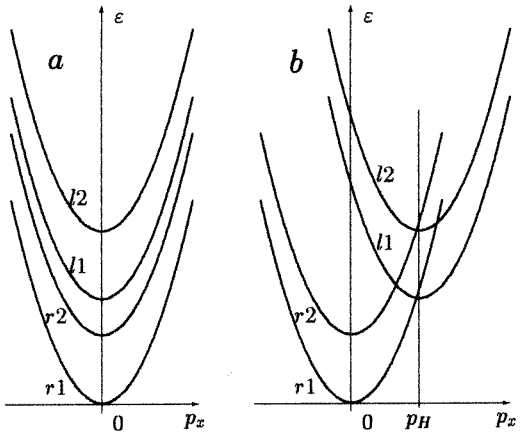

Figure 2. The electron spectrum of parallel quantum wires: (*a*) without the magnetic field; (*b*) with the magnetic field applied along the direction of lateral confinement. The wires are formed into a double-quantum-well system by application of the lateral confinement potential along the *y* axis. Only two 1D subbands for each layer are shown.

perpendicular to the tunnelling direction has been carried out in past years in two kinds of experiment. The first involves the measurement of the tunnelling relaxation rate of the photoexcited electrons in DQWs by means of time-resolved spectroscopy [5]. The second involves the measurement of the tunnel current between the 2D layers using separate contacts to each layer [4], or a gated-bridge technique [6]. Quite recently, an experimental study of the tunnelling between quasi-1D states in the magnetic field has been reported [3]. Both experimental data [4, 6] and theoretical calculations [6, 7] show that the tunnelling conductance of the DQWs appears to be insensitive to the scattering rates over a wide region of the magnetic fields. This remarkable behaviour confirms the non-dissipative tunnelling concept stated above. However, theoretical investigation of the problem is, in our opinion, still not sufficient. Existing calculations [6, 7] describe tunnelling between 2D electron layers only in the linear regime, where the tunnel current is characterized by the ohmic tunnelling conductance. These calculations refer to the proper kind of tunnelling experiment concerning measurements of the current in systems with separate contacts. As we demonstrate in this work, non-dissipative tunnelling also manifests itself in another kind of experiment [5], via the magnetic field dependence of the tunnelling relaxation rate of photoexcited electrons. As far as we know, quantitative explanation of these data is lacking. Non-dissipative tunnelling between quasi-1D electron states has not been indicated, although a model calculation of the tunnel current between the quantum wires has been presented [3].

The aims of this paper are: (i) to describe the tunnelling in the low-dimensional structures in the framework of a unified approach using Green function formalism; (ii) to derive expressions describing the tunnelling rate and tunnel current in the non-dissipative regime; and (iii) to compare results of calculations using these expressions with the existing experimental data on the tunnelling relaxation rate of photoexcited electrons in DQWs [5] and on the tunnel current in the independently contacted DQWs [4] and quantum wires [3]. Below, in sections 2 and 3, we develop a general formalism for calculation of the tunnel current j and rate of tunnelling ν, and apply it to the 2D and quasi-1D cases. In section 4 we derive the scattering-independent expressions for ν and j (respectively) using results from the previous sections, and present a comparison with the experiments.

2. General formalism

In consideration of the two-layer system, we use a basis of the l- and r-orbitals ($|l\rangle$ and $|r\rangle$, respectively). In this basis, the pair of tunnel-coupled electron states is described by the 2×2 matrix Hamiltonian

$$\begin{vmatrix} h_l & T \\ T & h_r \end{vmatrix}$$
$$h_l = \left[(\hat{p}_x - p_H)^2 + \hat{p}_y^2\right]/2m + \Delta_H + U_l(x, y) + W_l(y) \tag{1}$$
$$h_r = \left[\hat{p}_x^2 + \hat{p}_y^2\right]/2m + U_r(x, y) + W_r(y)$$

where T is the tunnelling matrix element, which is assumed to be independent of the magnetic field, $\hat{p}_x$ and $\hat{p}_y$ are the momentum operators, $U_{l,r}(x, y)$ are the random 2D potentials acting on the electrons in the l- and r-layers, and $W_{l,r}(y)$ are the lateral confinement potentials for these layers (introduction of these potentials allows one to describe a transition from the 2D to quasi-1D motion and to write expressions for ν and j in both of these cases in a unified way). The effect of the magnetic field is described by the characteristic momentum shift $p_H = |e|HZ/c$ and renormalized level splitting Δ_H, where

$H = |\boldsymbol{H}|$, e is the electron charge, c is the velocity of light,

$$Z = \langle r|z|r\rangle - \langle l|z|l\rangle \tag{2}$$

is the distance between the centres of the orbitals $|l\rangle$ and $|r\rangle$ in the right-hand and left-hand layers, and [8]

$$\Delta_H = \Delta + \frac{e^2H^2}{2mc^2}\left[\langle l|z^2|l\rangle - \langle r|z^2|r\rangle - \langle l|z|l\rangle^2 + \langle r|z|r\rangle^2\right]. \tag{3}$$

In order to describe the tunnelling probability, we introduce the electron density matrix and express its non-diagonal component $\tilde{\rho}_t$ through the diagonal components ρ_{lt} and ρ_{rt} according to [9] ($\delta \to +0$):

$$\tilde{\rho}_t = \frac{\mathrm{i}T}{\hbar}\int_{-\infty}^{t} \mathrm{d}t'\ \mathrm{e}^{\delta t'} \exp[-\mathrm{i}h_l(t-t')/\hbar][\rho_{lt'} - \rho_{rt'}] \exp[\mathrm{i}h_r(t-t')/\hbar]. \tag{4}$$

The diagonal components ρ_{jt} (here and below the subscript j denotes an l- or r-layer) are described by the closed system of equations ($j \neq j'$)

$$\frac{\partial \rho_{jt}}{\partial t} + \frac{\mathrm{i}}{\hbar}\left[h_j, \rho_{jt}\right] + \left(\frac{T}{\hbar}\right)^2 \int_{-\infty}^{t} \mathrm{d}t'\ \mathrm{e}^{\delta t'} \times \left\{\exp[-\mathrm{i}h_j(t-t')/\hbar][\rho_{jt'} - \rho_{j't'}] \exp[\mathrm{i}h_{j'}(t-t')/\hbar] + \mathrm{HC}\right\} = 0. \tag{5}$$

Below we assume that T is much smaller than the mean electron energy and collision broadening energy $\hbar/\tau$, and make the calculation in the lowest order of T^2. (In the opposite case, the electron states near the tunnelling resonance are hybridized, and description of the tunnelling becomes more complex.) Considering the case of tunnelling relaxation of the photoexcited electrons (see [5] and references therein) we obtain the balance equation $\mathrm{d}n_l(t)/\mathrm{d}t = -\nu n_l(t)$, which describes the decrease of the electron concentration in the l-layer $n_l(t)$ due to the tunnelling to the r-layer. The opposite current is neglected since we assume that the r-layer states are unpopulated. The observable value, the tunnelling rate ν, is obtained directly after transformation of equation (5) to the balance equation:

$$\nu = \frac{2\pi T^2}{\hbar}\left\langle \sum_{\lambda\lambda'} |(l\lambda|r\lambda')|^2\, \delta(\varepsilon_{l\lambda} - \varepsilon_{r\lambda'})\, f_{l\lambda}\right\rangle \Bigg/ \left\langle \sum_{\lambda} f_{l\lambda}\right\rangle \tag{6}$$

where the microscopic states $|j\lambda)$ and their energies $\varepsilon_{j\lambda}$ are determined from the eigenvalue problem $h_j|j\lambda) = \varepsilon_{j\lambda}|j\lambda)$, $f_{j\lambda}$ are the distribution functions, and $\langle ... \rangle$ means statistical averaging over the random potentials $U_j(x, y)$. In the systems with separate contacts, the observable value is the density of the tunnel current j, which is determined by the operator $2\mathrm{i}|e|T(\tilde{\rho}_t^+ - \tilde{\rho}_t)/(\hbar S)$ (S is the normalization area). Using equation (4), we obtain

$$j = \frac{4\pi|e|T^2}{\hbar S}\left\langle \sum_{\lambda\lambda'} |(l\lambda|r\lambda')|^2\, \delta(\varepsilon_{l\lambda} - \varepsilon_{r\lambda'})\,[f_{l\lambda} - f_{r\lambda'}]\right\rangle. \tag{7}$$

In the case of quasi-equilibrium, when the distribution functions depend only on the energies ($f_{j\lambda} = f_j(\varepsilon_{j\lambda})$), the above-presented formalism allows us to rewrite equations (6) and (7) through the Green functions of the electrons in the following way:

$$\nu = \frac{2\pi T^2}{\hbar}\int \mathrm{d}\varepsilon\, f_l(\varepsilon) \int \mathrm{d}x \int \mathrm{d}y \int \mathrm{d}x' \int \mathrm{d}y' \left\langle G_{\varepsilon l}(xy, x'y')G_{\varepsilon r}(x'y', xy)\right\rangle \times \left[\int \mathrm{d}\varepsilon\, f_l(\varepsilon) \int \mathrm{d}x \int \mathrm{d}y\, \langle G_{\varepsilon l}(xy, xy)\rangle\right]^{-1} \tag{8}$$

$$j = \frac{4\pi|e|T^2}{\hbar S^2}\int \mathrm{d}\varepsilon \int \mathrm{d}x \int \mathrm{d}y \int \mathrm{d}x' \int \mathrm{d}y' \left\langle G_{\varepsilon l}(xy, x'y')G_{\varepsilon r}(x'y', xy)\right\rangle [f_l(\varepsilon) - f_r(\varepsilon)]. \tag{9}$$

In the following section we apply these expressions to the two-dimensional and one-dimensional problems.

3. Tunnelling in two-dimensional and one-dimensional systems

Below, taking into account the ordinary experimental conditions, we calculate the tunnelling rate of photoexcited electrons using a non-degenerate distribution $f_j(\varepsilon) \sim \exp(-\varepsilon/T_e)$ with the effective temperature T_e. For the same reason, the current j is calculated by the use of degenerate distributions $f_j(\varepsilon) = \Theta(\varepsilon_{Fj} - \varepsilon)$; in this case we can also introduce the applied bias V defined by $|e|V = \varepsilon_{Fl} - \varepsilon_{Fr}$. For the sake of simplicity, we carry out the averaging in equations (8) and (9) assuming that the potentials $U_l(x, y)$ and $U_r(x, y)$ are statistically independent. In the calculation of ν and j—separately for the 2D and quasi-1D situations—it is convenient to write the Green functions from equations (8) and (9) in the momentum representation. As a result, both the tunnelling rate and the current between the 2D layers are expressed through the one-particle causal Green functions $G^{(2D)}_{\varepsilon l}(\boldsymbol{p})$ as follows:

$$\nu_{2D} = \frac{2\pi T^2}{\hbar}\int \mathrm{d}\varepsilon\ \exp(-\varepsilon/T_e)\int \frac{\mathrm{d}\boldsymbol{p}}{(2\pi\hbar)^2}\ G^{(2D)}_{\varepsilon l}(\boldsymbol{p})G^{(2D)}_{\varepsilon r}(\boldsymbol{p}) \times\left[\int \mathrm{d}\varepsilon\ \exp(-\varepsilon/T_e)\int \frac{\mathrm{d}\boldsymbol{p}}{(2\pi\hbar)^2}\ G^{(2D)}_{\varepsilon l}(\boldsymbol{p})\right]^{-1} \tag{10}$$

$$j_{2D} = \frac{4\pi|e|T^2}{\hbar}\int_{\varepsilon_{Fr}}^{\varepsilon_{Fl}} \mathrm{d}\varepsilon \int \frac{\mathrm{d}\boldsymbol{p}}{(2\pi\hbar)^2}\ G^{(2D)}_{\varepsilon l}(\boldsymbol{p})G^{(2D)}_{\varepsilon r}(\boldsymbol{p}) \tag{11}$$

where $\boldsymbol{p} = (p_x, p_y)$ is the 2D momentum, and

$$G^{(2D)}_{\varepsilon j}(\boldsymbol{p}) = \pi^{-1}\,\mathrm{Im}\left[\varepsilon_j(\boldsymbol{p}) - \varepsilon - \Sigma^{(2D)}_{\varepsilon j}(\boldsymbol{p})\right]^{-1}. \tag{12}$$

The electron spectra in the r- and l-wells (shown in figure 1) are obtained from the eigenvalue problem for Hamiltonian (1) in the absence of the random potentials and confinement potentials:

$$\varepsilon_l(\boldsymbol{p}) = \Delta_H + [(p_x - p_H)^2 + p_y^2]/2m \qquad \varepsilon_r(\boldsymbol{p}) = [p_x^2 + p_y^2]/2m. \tag{13}$$

Similar expressions of ν and j in the case of tunnelling between the quasi-1D layers are derived using the (p_x, n) representation, where n is the quantum number for the lateral confinement eigenstates. We obtain

$$\nu_{1D} = \frac{2\pi T^2}{\hbar}\int \mathrm{d}\varepsilon\ \exp(-\varepsilon/T_e)\sum_{nn'}\Phi_{nn'}\int \frac{\mathrm{d}p_x}{2\pi\hbar}\ G^{(1D)}_{\varepsilon l n}(p_x)G^{(1D)}_{\varepsilon r n'}(p_x) \times\left[\int \mathrm{d}\varepsilon\ \exp(-\varepsilon/T_e)\sum_{n}\int \frac{\mathrm{d}p_x}{2\pi\hbar}\ G^{(1D)}_{\varepsilon l n}(p_x)\right]^{-1} \tag{14}$$

$$j_{1D} = \frac{4\pi|e|T^2}{\hbar}\int_{\varepsilon_{Fr}}^{\varepsilon_{Fl}} \mathrm{d}\varepsilon\ \sum_{nn'}\Phi_{nn'}\int \frac{\mathrm{d}p_x}{2\pi\hbar}\ G^{(1D)}_{\varepsilon l n}(p_x)G^{(1D)}_{\varepsilon r n'}(p_x) \tag{15}$$

and

$$G^{(1D)}_{\varepsilon jn}(p_x) = \pi^{-1}\,\mathrm{Im}\left[\varepsilon_{jn}(p_x) - \varepsilon - \Sigma^{(1D)}_{\varepsilon jn}(p_x)\right]^{-1}. \tag{16}$$

The electron spectra corresponding to the r- and l-layers (see figure 2) are given by the expressions

$$\varepsilon_{ln}(p_x) = \Delta_H + E^l_n + (p_x - p_H)^2/2m \qquad \varepsilon_{rn}(p_x) = E^r_n + p_x^2/2m. \tag{17}$$

In equations (14) and (15)

$$\Phi_{nn'} = \left|\int \mathrm{d}y\ \varphi^l_n(y)\varphi^r_{n'}(y)\right|^2$$

is the squared overlap integral of the lateral confinement eigenstates, while E^l_n and E^r_n in equation (17) are the lateral quantization energies. Both $\varphi^j_n(y)$ and E^j_n are determined from the eigenvalue problem $[\hat{p}_y^2/2m + W_j(y) - E^j_n]\varphi^j_n(y) = 0$. A calculation of the self-energies $\Sigma^{(2D)}_{\varepsilon j}(\boldsymbol{p})$ and $\Sigma^{(1D)}_{\varepsilon jn}(p_x)$ in equations (12) and (16) requires explicit description of the scattering. However, if the typical energy of the electrons (the temperature or Fermi energy) is much larger than the self-energies, we can use a collisionless approximation, where the imaginary parts of the self-energies go to zero and the real parts are neglected as a small renormalization of the energy spectra. From the physical point of view, this approach describes the non-dissipative tunnelling regime and leads to scattering-independent expressions for the tunnelling rate and tunnel current, which are valid over a wide interval of the magnetic fields and other parameters. These expressions are derived and analysed in the following section.

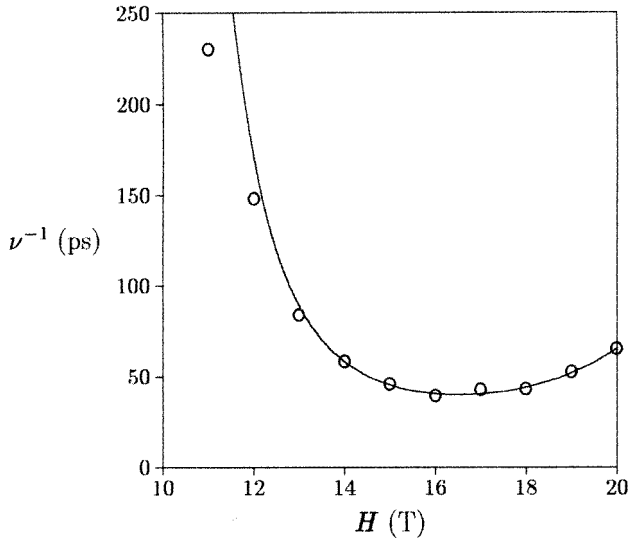

Figure 3. The dependence of the tunnelling time in the GaAs/$Ga_{0.65}Al_{0.35}$As/GaAs DQWs (5 nm/6 nm/10 nm) on the magnetic field H. The solid line shows the results from the calculation using equation (18); the points are taken from experiment [5].

4. Results

4.1. The tunnelling relaxation rate

Application of the collisionless approximation to equation (12) gives $G_{\varepsilon j}^{(2D)}(\boldsymbol{p}) \simeq \delta(\varepsilon_j(\boldsymbol{p}) - \varepsilon)$. After substitution of this formula into equation (10), we obtain

$$\nu_{2D} = \frac{\sqrt{\pi}T^2}{\hbar\sqrt{T_e\varepsilon_H}} \exp\left[-\frac{(\varepsilon_H - \Delta_H)^2}{4\varepsilon_H T_e}\right] \tag{18}$$

where $\varepsilon_H = p_H^2/2m$. This formula describes resonant-like dependence of the tunnelling rate on the magnetic field as well as on the level splitting. The rate is highest when $\varepsilon_H \simeq \Delta_H$, i.e., when the spectrum intersection line goes through the minimum of the l well spectrum. As we shift out of this resonance, the number of electrons near the intersection becomes smaller, and the tunnelling rate decreases exponentially. We also note the asymmetry of ν_{2D} as a function of the magnetic field.

A dependence of this kind has been recently observed experimentally [5] in asymmetric GaAs/$Ga_{0.65}Al_{0.35}$As DQWs. In order to demonstrate that the non-dissipative tunnelling regime has been really realized in this experiment, we have compared equation (18) with the experimental curve of the tunnelling time ν^{-1} versus H. The result (see figure 3) is described by the following parameters: splitting energy Δ, tunnelling matrix element T, and electron temperature T_e. The value of Δ fixes the position of the resonance, T_e (under fixed Δ), and determines its width, while T (under fixed Δ and T_e) gives the tunnelling time in the resonance. A good agreement is achieved at $\Delta = 73$ meV, $T = 0.425$ meV and $T_e = 63$ K. For comparison, an estimate in the square-well approximation gives $\Delta \simeq 60$ meV and $T \simeq 0.2$ meV, while the experimental data provide $T_e \simeq 50$ K. At small H, the experimental values of ν^{-1} are smaller than the theoretical ones. This is not surprising, since far from the resonance the number of electrons able to perform non-dissipative tunnelling is exponentially small, and one should use the more general equation (10) instead of equation (18). Nevertheless, when T_e exceeds the collision broadening energy, equation (18) describes the experimental data in the vicinity of the resonance quite well.

From equation (14) with $G_{\varepsilon jn}^{(1D)}(p_x) \simeq \delta(\varepsilon_{jn}(p_x) - \varepsilon)$, we find the rate of tunnelling in the quantum wire states:

$$\nu_{1D} = \frac{\sqrt{\pi}T^2}{\hbar\sqrt{T_e\varepsilon_H}} \sum_{nn'} \Phi_{nn'} \exp\left(-\frac{E_n^l}{T_e}\right) \exp\left[-\frac{(\varepsilon_H - \Delta_H - E_n^l + E_{n'}^r)^2}{4\varepsilon_H T_e}\right] \times \left[\sum_n \exp\left(-\frac{E_n^l}{T_e}\right)\right]^{-1} \tag{19}$$

which behaves in a similar way to ν_{2D}. We stress that in the case of equal lateral potentials in both wells ($W_l(y) = W_r(y)$) we have $E_n^l = E_n^r$ and $\Phi_{nn'} = \delta_{nn'}$, so the tunnelling relaxation rate ν_{1D} appears to be equal to ν_{2D}. As far as we know, tunnelling between the wires has not been studied by means of time-resolved spectroscopy, though time-resolved investigation of the electron energy relaxation in a single wire has already been reported [10].

4.2. The tunnel current

The non-dissipative tunnel current between 2D systems is found after application of the collisionless approximation to equation (11):

$$j_{2D} = \frac{|e|T^2 m}{\pi\hbar^3\varepsilon_H}\left\{\sqrt{4\varepsilon_H(\varepsilon_{Fr}+|e|V)-(\Delta_H+\varepsilon_H)^2}-\sqrt{4\varepsilon_H\varepsilon_{Fr}-(\Delta_H+\varepsilon_H)^2}\right\} \tag{20}$$

where the square roots are assumed to be equal to zero when the expressions under them are negative. Equation (20) describes a non-zero current when the line of the spectrum intersection appears in the energy interval between ε_{Fr} and ε_{Fl}. There can be two kinds of current–voltage characteristic $j_{2D}(V)$. For $\varepsilon_{Fr} < (\Delta_H+\varepsilon_H)^2/4\varepsilon_H$ we have a square-root dependence with the threshold at $|e|V = (\Delta_H+\varepsilon_H)^2/4\varepsilon_H - \varepsilon_{Fr}$, i.e. the non-dissipative current is abruptly turned on with the increase of V. For the opposite inequality we have a linear dependence of j_{2D} on V for small voltage (the ohmic case). The dependence of j_{2D} on the level splitting Δ is more complex. However, in conditions where the number of electrons in the r-layer is small and the back current (the second square root in equation (20)) may be neglected, this dependence is described by a semi-ellipse with a maximum at $\Delta_H = \varepsilon_H$.

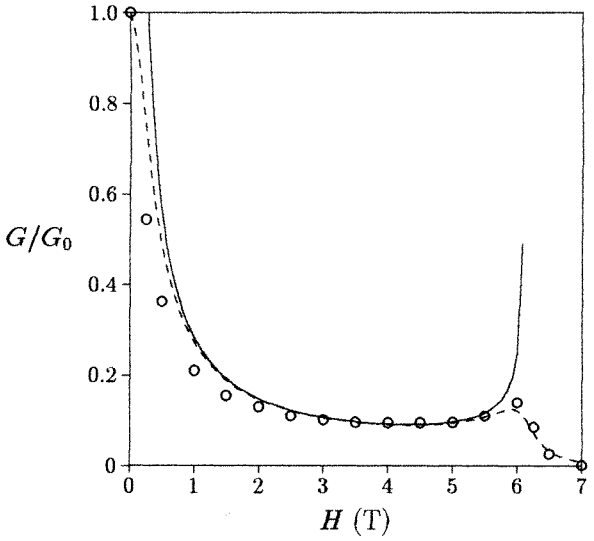

Figure 4. The dependence of the tunnelling conductance G in the GaAs/$Ga_{0.65}Al_{0.35}$As/GaAs DQWs (13 nm/7 nm/13 nm) on H at $\Delta = 0$. The solid and dashed lines correspond to calculations using equations (20) and (11), respectively. The experimental points are taken from [4].

In the ohmic case, one can introduce the interlayer conductance G according to $G = (j_{2D}/V)_{V\to 0}$. The conductance has been calculated in [7] using the Kubo formalism, and an expression for G in the non-dissipative regime has been derived. This calculation qualitatively described the experimental [4] dependence of G on the magnetic field and level splitting, but a detailed comparison with the experiment has not been presented. In figure 4 we plot the normalized conductance versus the magnetic field calculated with the use of the experimental parameters from [4] (points correspond to experimental data). The dashed line corresponds to a calculation using the more general equation (11), where we

estimate $\Sigma_{\varepsilon j}^{(2D)}(\boldsymbol{p}) \simeq \mathrm{i}\overline{h}/(2\tau_j)$ and τ_j is the scattering time in the Fermi surface of the jth well (this approach is correct since $\varepsilon_{Fj} \gg \overline{h}/\tau_j$). We assume symmetrical scattering $\tau_l = \tau_r$ and choose $\overline{h}/\tau_l \simeq 1$ meV in order to match the height of the non-dissipative 'plateau' with the height of the resonance at $H = 0$. With this single fitting parameter, a reasonable agreement with the experiment is obtained.

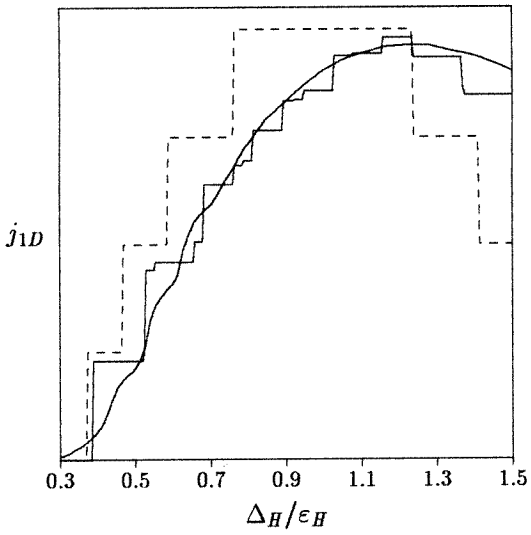

Figure 5. The tunnel current j_{1D} (arbitrary units) of the tunnelling between the quantum wires as a function of the level splitting Δ at $H = 10$ T (the parameters are taken from [3] and described in the text). The smooth solid line shows the experimental dependence [3].

Let us consider the non-dissipative current between the quantum wires (quasi-1D systems). In the collisionless approximation, equation (15) transforms to

$$j_{1D} = \frac{2|e|T^2 m}{\overline{h}^2 p_H} \sum_{nn'} \Phi_{nn'} \Theta\left[4\varepsilon_H(\varepsilon_{Fl} - E^r_{n'}) - (E^l_n - E^r_{n'} + \Delta_H + \varepsilon_H)^2\right] \times \Theta\left[(E^l_n - E^r_{n'} + \Delta_H + \varepsilon_H)^2 - 4\varepsilon_H(\varepsilon_{Fr} - E^r_{n'})\right]. \tag{21}$$

This formula shows that the current is non-zero when at least one point of the spectrum intersection (see figure 2(*b*)) is situated in the energy interval between ε_{Fr} and ε_{Fl}. The current demonstrates a step-like growth (or decrease) as a function of the magnetic field, applied voltage and level splitting when a new intersection point comes in (or out of) this interval. To demonstrate this remarkable behaviour, we have calculated j_{1D} as a function of the level splitting at constant magnetic field $H = 10$ T for the following experimental conditions [3]: the l-layer (emitter) is uniformly occupied and $\varepsilon_{Fl} - \Delta_H = 6$ meV; the r-layer is unoccupied ($\varepsilon_{Fr} = 0$); the lateral confinement potentials in the wells are parabolic and $W_j(y) = m\Omega_j^2 y^2/2$, $\overline{h}\Omega_l = 1.5$ meV, $\overline{h}\Omega_r = 3.5$ meV; the effective interlayer separation $Z = 20$ nm. The dependence is shown in figure 5 by the solid 'staircase' line. The dashed staircase line shows the same dependence for a simplified situation, when $\overline{h}\Omega_l = \overline{h}\Omega_r = 1.5$ meV and the tunnelling occurs only between the subbands with equal numbers ($n' = n$). Since there are only four subbands below the Fermi level in the emitter, the total number of steps is four. The case of non-equal Ω_j shows a more complex picture of steps, but the highest steps again correspond to the transitions with $n' = n$. The steps are clearly visible in the experimental curve from [3], which is also plotted in figure 5. The fit between the experimental and theoretical data in figure 5 is achieved by adjusting the values of the threshold voltage and maximum-current voltage to the proper theoretical values of

Δ_H. Also, the maximum current is fitted to its experimental value $j_{1D}L \simeq 0.8$ nA, where $L \simeq 600$ nm is the wire length [3]. This fit allows one to extract the value of the tunnelling matrix element $T \simeq 0.016$ meV from the experimental data. A value of the same order is obtained from a numerical estimate using parameters for the structure investigated.

A more detailed agreement between the experimental and theoretical data may be achieved when a scattering is taken into consideration. As follows from equation (15), the scattering should lead to some broadening of the sharp steps in the staircase dependence shown in figure 5. In order to explain their experiment, the authors of [3] have carried out a calculation using a formula similar to equation (15), where the product of Green functions is replaced by a Lorentzian. This modelling approach describes broadening of the experimental curves, but it is not concerned with detailed consideration of the scattering. On the other hand, the simple scattering-independent analytical expression (21) not only satisfactorily explains the experiment [3], but also demonstrates the importance of the collisionless approach in calculation of the tunnel current in quasi-1D systems.

In conclusion, application of the magnetic field perpendicular to the direction of the tunnelling allows one to realize the non-dissipative interlayer tunnelling regime in low-dimensional systems. This regime exists due to the field-induced intersection of the parabolic branches of the electron spectra belonging to the different layers. The tunnel current in these conditions is determined only by the magnetic field, level splitting, tunnelling matrix element, and energy distribution of the electrons. As we tried to show in this study, this behaviour is consistent with measurements of the tunnelling relaxation rate of the photoexcited electrons in DQWs as well as with measurements of the tunnel current between independently contacted 2D and quasi-1D layers.

Acknowledgment

This work was supported in part by Grant No U65200 from the Joint Fund of the Government of the Ukraine and the International Science Foundation.

References

[1] Eisenstein J P 1992 *Superlatt. Microstruct.* **12** 107
Smoliner J, Gornik E and Weimann G 1989 *Phys. Rev.* B **39** 12 937
[2] Kazarinov R F and Suris R A 1972 *Fiz. Tekh. Poluprov.* **6** 148
[3] Wang J, Beton P H, Mori N, Eaves L, Buhmann H, Mansouri L, Main P C, Foster T J and Henini M 1994 *Phys. Rev. Lett.* **73** 1146
Mori N, Beton P H, Wang J and Eaves L 1995 *Phys. Rev.* B **51** 1735
[4] Eisenstein J P, Gramila T J, Pfeiffer L N and West K W 1991 *Phys. Rev.* B **44** 6511
[5] Heberle A P, Oestereich M, Haacke S, Rühle W W, Maan J C and Köhler K 1994 *Phys. Rev. Lett.* **72** 1522
[6] Simmons J A, Lyo S K, Klem J F, Sherwin M E and Wendt J R 1993 *Phys. Rev.* B **47** 15 741
[7] Zheng L and MacDonald A H 1993 *Phys. Rev.* B **47** 10 619
[8] Raichev O E and Vasko F T 1995 *Phys. Rev.* B **52** at press
[9] Raichev O E and Vasko F T 1994 *Superlatt. Microstruct.* **15** 133
[10] Mayer G, Prins F E, Lehr G, Schweizer H, Leier H, Maile B E, Straka J, Forchel A and Weimann G 1993 *Phys. Rev.* B **47** 4060